

# High-temperature stabilized anatase TiO<sub>2</sub> from an aluminum-doped TiCl<sub>3</sub> precursor†

Sujith Perera and Edward G. Gillan\*

Received (in Cambridge, UK) 30th August 2005, Accepted 5th October 2005

First published as an Advance Article on the web 3rd November 2005

DOI: 10.1039/b512148e

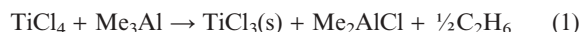
The solid-state hydrolysis and air calcination of aluminum-doped TiCl<sub>3</sub> leads to crystalline anatase TiO<sub>2</sub> that is stable on heating to 1000 °C, in contrast to control studies with related AlCl<sub>3</sub> and TiCl<sub>3</sub> physical mixtures that produce rutile TiO<sub>2</sub> under the same conditions.

Group 4 (Ti, Zr, Hf) oxides each have a thermodynamically stable MO<sub>2</sub> phase, and at least one phase that is kinetically stable at low temperatures (<500 °C) and converts to thermodynamic or higher temperature kinetic phases upon heating. In the zirconium system, a tetragonal ZrO<sub>2</sub> phase crystallizes from amorphous precipitates and converts to monoclinic and cubic phases upon heating above ~800–1200 °C.<sup>1</sup> The monoclinic is the thermodynamically stable phase at room temperature. Many studies have shown that small amounts of secondary metals (<10%) such as Ca, Y and Ce will allow cubic or tetragonal ZrO<sub>2</sub> phases to be formed at relatively low temperatures and retained during high temperature heating (known as stabilized zirconias).<sup>2</sup> Similar phase stabilization processes occur in the HfO<sub>2</sub> system.

The smallest Group 4 element, titanium, also forms several TiO<sub>2</sub> structures. There are numerous solution routes which produce nanocrystalline or amorphous precipitates that crystallize upon heating to low-temperature anatase TiO<sub>2</sub> phase (body-centered tetragonal) and transform to the thermodynamically stable rutile TiO<sub>2</sub> form (primitive tetragonal) upon extended heating above 500 °C.<sup>3</sup> There is an example of direct anatase formation by ultrasound assisted hydrolysis.<sup>4</sup> Since anatase TiO<sub>2</sub> is generally more photocatalytically active than the rutile form,<sup>5</sup> it is desirable to produce crystallographically-ordered anatase structures and retard phase conversion. There are examples of anatase stabilization up to 800 °C using sulfate ions,<sup>6</sup> Al or Ga,<sup>7</sup> and Ce or Cu.<sup>8</sup> This report describes an observation that TiCl<sub>3</sub> containing trace aluminum, synthesized by an organometallic exchange reaction, can be air-hydrolyzed and calcined at 1000 °C to produce crystalline stabilized anatase TiO<sub>2</sub>. This is in clear contrast to several control reactions with different types of TiCl<sub>3</sub> that only produce the rutile TiO<sub>2</sub>.

The organometallic synthetic reduction of TiCl<sub>4</sub> by Me<sub>3</sub>Al in heptane at elevated temperatures is reported to produce β-TiCl<sub>3</sub> (hexagonal, JCPDS #29–1358).<sup>9</sup> In the current study, this reaction

produced crystalline brown β-TiCl<sub>3</sub> after drying and heating under vacuum, as determined by powder X-ray diffraction (XRD). The balanced chemical reaction in heptane is shown in eqn. 1 (see ESI for experimental details†). All components are dissolved unless noted.



ICP-AE analysis showed that the as-synthesized TiCl<sub>3</sub> contained a few percent of aluminum (~97 : 3, Ti : Al molar ratio). A portion of this material was heated in an evacuated glass ampoule at 350 °C for 16 h to produce dark purple α-TiCl<sub>3</sub> by XRD (hexagonal, JCPDS #29–1357), with a slightly lower residual aluminum content due to the transport of volatile aluminum species (Table 1). The TiCl<sub>3</sub> materials from the organometallic synthesis as-synthesized and after sublimation are denoted TiCl<sub>3</sub>(om) and TiCl<sub>3</sub>(om, sub), respectively. High purity α-TiCl<sub>3</sub> is most commonly synthesized *via* hydrogen reduction of TiCl<sub>4</sub> on a heated tungsten filament.<sup>10</sup> A commercial high purity α-TiCl<sub>3</sub> (99.9%) sample, TiCl<sub>3</sub>(com), was used as a control and has essentially no detectable aluminum content by ICP-AE analysis (<0.05 wt% at baseline detection limits). Since TiCl<sub>3</sub> is one component of widely used Ziegler–Natta polymerization catalysis, another common and inexpensive form is a 3TiCl<sub>3</sub>/AlCl<sub>3</sub> mixture that is usually formed by the reaction of TiCl<sub>4</sub> and Al powder.<sup>9a</sup> A commercial sample of this physical mixture of the individual metal trichlorides, TiCl<sub>3</sub>(com-25% Al), was heated under vacuum at 350 °C to sublime the AlCl<sub>3</sub> away from the TiCl<sub>3</sub> phase (TiCl<sub>3</sub>(com-25% Al, sub)), thus completing a set of five different TiCl<sub>3</sub> samples for oxidation to TiO<sub>2</sub>. Each of their Ti and Al contents and crystalline phases are listed in Table 1, and the data shows that the sublimed materials still contain measurable amounts of aluminum. Table S1 (ESI material†) lists ICP-AE weight percent data.

In each experiment, approximately 100 mg of the TiCl<sub>3</sub> precursor was loaded into a glass vial in an inert atmosphere glovebox and then placed in air overnight (~15 h) to allow room temperature hydrolysis and oxidation to slowly occur. The TiCl<sub>3</sub> precursors were well-behaved upon air exposure, and gained weight and lost most of their color. Room temperature and relative humidity were not regulated but were typically around 27 °C and 60% RH in the laboratory. Though the air reaction was a fairly uncontrolled process, it was likely to include some HCl formation and Ti(III) to Ti(IV) oxidation. It is reasonable that Ti and Al local mixing in the chloride precursor is retained after hydrolysis. The hydrolyzed materials were further oxidized and calcined in air in an open horizontal tube furnace using a rapid 30 min ramp to 1000 °C and holding it at this temperature for 2 h.

Department of Chemistry, University of Iowa and the Optical Science and Technology Center, Iowa City, 52242-1294, Iowa, USA.  
E-mail: edward-gillan@uiowa.edu; Fax: (+1) 319 335-1270;  
Tel: (+1) 319 335-1308

† Electronic Supplementary Information (ESI) available: Detailed experimental procedures, ICP and weight change data, and SEM images for calcined TiO<sub>2</sub> from TiCl<sub>3</sub>(com-25% Al) and TiCl<sub>3</sub>(com-25% Al, sub). See DOI: 10.1039/b512148e

**Table 1** Precursor and product data for TiCl<sub>3</sub> hydrolysis and oxidation experiments

Sample <sup>a</sup>	TiCl <sub>3</sub> precursor Ti : Al molar ratio <sup>b</sup>	TiO <sub>2</sub> product Ti : Al molar ratio <sup>b</sup>	TiO <sub>2</sub> phases a : r (wt%) <sup>e</sup>	TiO <sub>2</sub> crystallite size/nm
β-TiCl <sub>3</sub> (om)	96.8 : 3.2	98.5 : 1.5	83 : 17	a = 100, r > 300
α-TiCl <sub>3</sub> (om, sub)	97.3 : 2.7	98.8 : 1.2	55 : 45	a, r = 130
α-TiCl <sub>3</sub> (com)	99.7 : <0.3 <sup>c</sup>	100 : 0 <sup>c</sup>	0 : 100	100
α-TiCl <sub>3</sub> (com-25% Al) <sup>d</sup>	74.4 : 25.6	78.3 : 21.7	0 : 100	130
α-TiCl <sub>3</sub> (com-25% Al, sub)	97.4 : 2.6	98.6 : 1.4	0 : 100	230

<sup>a</sup> TiCl<sub>3</sub> phase (α or β) determined by XRD; om = organometallic synthesis, com = commercial, sub = sublimed. <sup>b</sup> From ICP-AE; molar ratio normalized to 100%. <sup>c</sup> Al at baseline detection limits. <sup>d</sup> No crystalline AlCl<sub>3</sub> was observed. <sup>e</sup> Wt% based on XRD peak ratio relationship using ref. 11 for anatase (a) and rutile (r) peaks near 25.5° and 27.5°, respectively.

A general overall reaction process for these two conversion steps is shown in eqn. 2.



The annealed TiO<sub>2</sub> products were examined by XRD, and phosphoric/sulfuric acid-dissolved samples were quantitatively analyzed by ICP-AE. Table 1 lists data on the titanium and aluminum molar ratios for each TiO<sub>2</sub> sample after calcination. Table S1 (ESI material†) also lists weight changes before and after room temperature hydrolysis and calcination.

The XRD results show that TiCl<sub>3</sub> synthesized *via* organometallic reduction oxidizes to predominantly anatase TiO<sub>2</sub> and retains most of this structure at 1000 °C (Fig. 1a). The weight percent anatase vs. rutile was calculated using published XRD peak intensity relationships (Table 1).<sup>11</sup> This degree of anatase phase stabilization is also retained during longer calcination periods at 1000 °C for 24 h. This result was reproduced by several samples, and the anatase phase was greater than 80 wt% in every case. When this TiCl<sub>3</sub>(om) precursor was heated under vacuum before hydrolysis (TiCl<sub>3</sub>(om, sub)), it produced less high temperature stabilized anatase than the TiCl<sub>3</sub>(om) sample (Fig. 1b). In sharp contrast, all other samples, even the ones with similar or greater

bulk aluminum contents, only produced crystalline rutile after 1000 °C heating (Fig. 1c–e). In addition, Al<sub>2</sub>O<sub>3</sub> (corundum) was observed in the calcined TiCl<sub>3</sub>(com-25% Al) product. The metal halide hydrolysis appears to be a necessary step because direct heating of TiCl<sub>3</sub>(om) sample in air to 1000 °C produced visible white smoke when the temperature reached 200 °C and the product was predominantly rutile with only 21 wt% of the anatase phase.

The annealed TiO<sub>2</sub> products are white aggregated solids that were easily ground into fine powders with a mortar and pestle. Estimates of crystallite sizes by XRD line broadening analyses are at or above 100 nm for all TiO<sub>2</sub> products (Table 1). Previous studies on unstabilized anatase report that crystallite grain growth above 15 nm leads to an irreversible conversion to rutile,<sup>12</sup> and similar observations have been made in ZrO<sub>2</sub> phase transformations.<sup>13</sup> Thus, another outcome of this work is that the anatase phase is stabilized at larger crystallite sizes than are usually observed in unstabilized systems.

The morphology of the stabilized anatase product is distinct from the rutile oxides. Scanning electron microscopy (SEM) images of anatase TiO<sub>2</sub> from TiCl<sub>3</sub>(om) show larger, roughly spherical particles (~2 μm) decorated with smaller ~50 nm faceted particles (Fig. 2a and 2b). The larger particles are observed to be hollow with wall thicknesses close to 100 nm. The rutile TiO<sub>2</sub> products from low aluminum content precursors have micron thick, plate-like morphologies that seem to be built-up of fused particles (Fig. 2c and 2d). In contrast, the high Al content

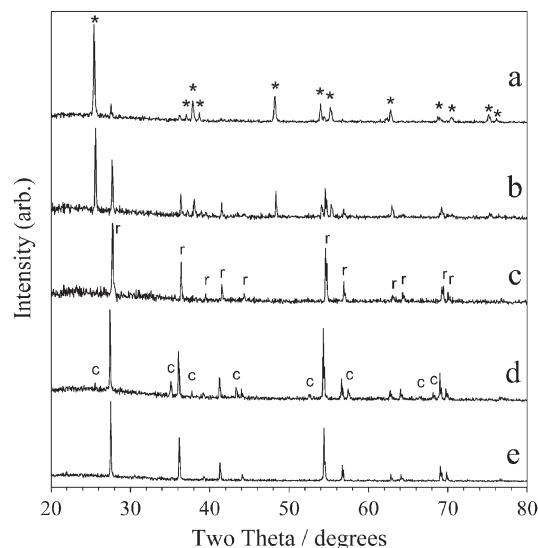


**Fig. 1** X-Ray diffraction data for hydrolyzed and annealed TiCl<sub>3</sub> precursors after solid air hydrolysis and 1000 °C calcination. (a) TiCl<sub>3</sub>(om), (b) TiCl<sub>3</sub>(om, sub), (c) TiCl<sub>3</sub>(com), (d) TiCl<sub>3</sub>(com-25% Al) and (e) TiCl<sub>3</sub>(com-25% Al, sub). \* indicates anatase peaks, r indicates rutile peaks and c indicates corundum (Al<sub>2</sub>O<sub>3</sub>) peaks.

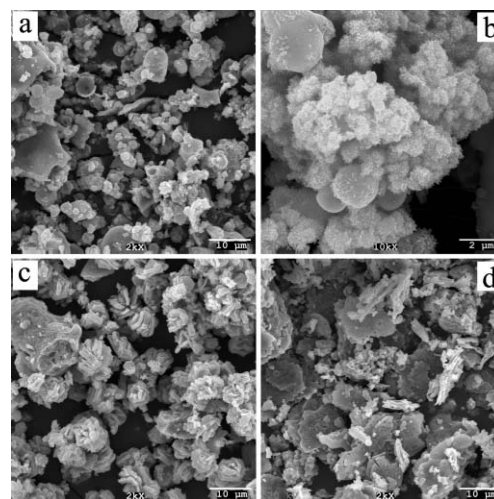


**Fig. 2** SEM images of TiO<sub>2</sub> from air hydrolyzed and calcined (a, b) TiCl<sub>3</sub>(om), (c) TiCl<sub>3</sub>(om, sub) and (d) TiCl<sub>3</sub>(com).

TiCl<sub>3</sub>(com-25% Al) precursor produced much larger grained 5–10 μm expansive continuous regions, possibly because of its high Al<sub>2</sub>O<sub>3</sub> content, along with clusters of smaller ~50 nm particles. When the AlCl<sub>3</sub> is sublimed away from this precursor, its calcined morphology reverts back to the plate-like shapes seen for similar low Al content products in Fig. 2 (ESI, Figure S1†).

Our working hypothesis as to why anatase phase stabilization only occurs for the TiCl<sub>3</sub> precursor from organometallic synthesis is that the small residual aluminum content in TiCl<sub>3</sub>(om) is probably more homogeneously-mixed at an atomic level in the bulk structure than it is in the macroscopically-separate phases found in commercial Ti/Al samples, e.g. TiCl<sub>3</sub>(com-25% Al, sub). The local bonding in TiCl<sub>3</sub> consists of distorted octahedra with all Cls shared between two Ti centers.<sup>14</sup> This is essentially the same as the AlCl<sub>3</sub> structure, and thus it is reasonable to presume that if Al is present during the TiCl<sub>4</sub> to TiCl<sub>3</sub> reduction and precipitation processes, small amounts of Al may be incorporated into Ti sites within the TiCl<sub>3</sub> structure. During hydrolysis, these would be intimately situated near other the titanium metals and form more homogeneously-mixed Al-containing TiO<sub>2</sub>, after calcination. This is consistent with other studies that show evidence of enhanced anatase stability up to 800 °C,<sup>6–8</sup> though the current work shows added stability to 1000 °C for extended periods of time. Semi-quantitative energy dispersive spectroscopy of this stabilized anatase product shows that residual chlorine is below baseline detection (<0.1 wt%).

Since there is less anatase formed from the sublimed TiCl<sub>3</sub>(om, sub) material, the phase of the starting TiCl<sub>3</sub> (α vs. β) along with the intimate mixing of aluminum might also play a role in the phase stabilization. Future work will spectroscopically compare the local aluminum and titanium bonding in the organometallic and commercial precursors and hydrolyzed samples to determine if there are clear structural distinctions that could explain why only the TiCl<sub>3</sub>(om) sample, with its trace aluminum, leads to high temperature stabilized anatase TiO<sub>2</sub>. The reasons are complex, since no anatase stabilization was observed when the system was overloaded with aluminum using TiCl<sub>3</sub>(com-25% Al).

The UV photodegradation of methylene blue (MB) by TiO<sub>2</sub> was investigated so as to test the relative photocatalytic abilities of the synthesized TiO<sub>2</sub> powders vs. a commercial TiO<sub>2</sub> standard (Degussa P25, ~20 nm particle size, 75% anatase, 25% rutile; see ESI information for details†). A MB solution without any oxide catalyst was degraded by only 6% after 20 min of UV exposure, while the anatase TiO<sub>2</sub> from TiCl<sub>3</sub>(om) and rutile TiO<sub>2</sub> from TiCl<sub>3</sub>(com) degraded the MB solution by 48% and 16%, respectively. The smaller particle size P25 standard showed nearly complete MB degradation in 15 min, but based on particle size differences, its relative surface area is likely to be several orders of magnitude higher than the anatase from TiCl<sub>3</sub>(om), which has an average particle size roughly five times larger than the P25 titania. Previous studies have also indicated that the presence of aluminum

dopants (<1 wt%) can decrease TiO<sub>2</sub> photocatalytic ability,<sup>7b,15</sup> while at high aluminum concentrations (~10 wt% Al) others have reported an increase in photocatalytic ability.<sup>7c</sup> It has also been concluded that surface adsorbed Al<sup>3+</sup> ions have improved organic surface cleaning during TiO<sub>2</sub> photocatalytic processes.<sup>16</sup>

In addition, recent reports have shown that lower valent Ti(III) residues in TiO<sub>2</sub> may also enhance visible absorption and photoactivity, something that may be accessible using a TiCl<sub>3</sub> precursor-based synthetic strategy.<sup>17</sup> Future studies will use the TiCl<sub>3</sub>(om) precursor in conjunction with other transition metals to generate stabilized anatase structures with lower energy light absorptions to increase their potential for visible light photocatalysis. In summary, an organometallic synthesis of β-TiCl<sub>3</sub> containing ~0.5 wt% aluminum yields predominantly stabilized anatase TiO<sub>2</sub> after air oxidation and calcination at 1000 °C. Particle and crystallite sizes are at or above 100 nm, which is much larger than sizes observed for unstabilized anatase TiO<sub>2</sub> systems.

The authors gratefully acknowledge the University of Iowa and National Science Foundation (CHE-0407753) for partial support of this research.

## Notes and references

- (a) R. Srinivasan, C. R. Hubbard, O. B. Cavin and B. H. Davis, *Chem. Mater.*, 1993, **5**, 27; (b) Y.-C. Zhang, S. Davison, R. Brusasco, Y.-T. Qian, K. Dwight and A. Wold, *J. Less-Common Met.*, 1986, **116**, 301.
- (a) R. C. Garvie, R. H. Hanink and R. T. Pascoe, *Nature*, 1975, **258**, 703; (b) R. P. Ingel and D. Lewis III, *J. Am. Ceram. Soc.*, 1986, **4**, 325.
- (a) K. I. Gnanasekar, V. Subramanian, J. Robinson, J. C. Jiang, F. E. Posey and B. Rambabu, *J. Mater. Res.*, 2002, **17**, 1507; (b) J. Ovenstone and K. Yanagisawa, *Chem. Mater.*, 1999, **11**, 2770.
- W. Huang, X. Tang, Y. Wang, Y. Kolytyn and A. Gedanken, *Chem. Commun.*, 2000, 1415.
- (a) A. Wold, *Chem. Mater.*, 1993, **5**, 280; (b) A. L. Linsebigler, G. Lu and J. T. Yates Jr., *Chem. Rev.*, 1995, **95**, 735.
- X. Bokhimi, A. Morales, O. Novaro, T. Lopez, O. Chimal, M. Asomoza and R. Gomez, *Chem. Mater.*, 1997, **9**, 2616.
- (a) L. E. Depero, A. Marino, B. Allieri, E. Bontempi, L. Sangaletti, C. Casale and M. Notaro, *J. Mater. Res.*, 2000, **15**, 2080; (b) B.-Y. Lee, S.-H. Park, M. Kang, S.-C. Lee and S.-J. Choung, *Appl. Catal., A*, 2003, **253**, 371; (c) M. Anpo, T. Kawamura, S. Kodama, K. Maruya and T. Onishi, *J. Phys. Chem.*, 1988, **92**, 438.
- R. F. de Fraias and C. Airolidi, *J. Non-Cryst. Solids*, 2005, **351**, 84.
- (a) F. Auremma, V. Busico, P. Corradini and M. Trifuoggi, *Eur. Polym. J.*, 1992, **28**, 513; (b) P. H. J. Moyer, *J. Polym. Sci.*, 1965, **3**, 209.
- W. L. Groeneveld, G. P. M. Leger, J. Wolters and R. Waterman, *Inorg. Synth.*, 1963, **7**, 45.
- R. A. Spurr and H. Myers, *Anal. Chem.*, 1957, **29**, 760.
- H. Zhang and J. F. Banfield, *J. Mater. Chem.*, 1998, **8**, 2073.
- R. C. Garvie, *J. Phys. Chem.*, 1978, **82**, 218.
- A. F. Wells, *Structural Inorganic Chemistry*, Clarendon Press, Oxford, 5th edn, 1990.
- W. Choi, A. Termin and M. R. Hoffmann, *J. Phys. Chem.*, 1994, **98**, 13669.
- M. I. Franch, J. Peral, X. Domenech and J. A. Ayllon, *Chem. Commun.*, 2005, 1851.
- I. N. Martyanov, S. Uma, S. Rodrigues and K. J. Klabunde, *Chem. Commun.*, 2004, 2476.